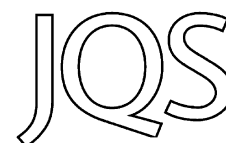


# Influence of tidal-range change and sediment compaction on Holocene relative sea-level change in New Jersey, USA



BENJAMIN P. HORTON,<sup>1,2\*</sup> SIMON E. ENGELHART,<sup>1,3</sup> DAVID F. HILL,<sup>4</sup> ANDREW C. KEMP,<sup>1,5</sup> DARIA NIKITINA,<sup>6</sup> KENNETH G. MILLER<sup>7</sup> and W. RICHARD PELTIER<sup>8</sup>

<sup>1</sup>Sea Level Research, Department of Earth and Environmental Science, University of Pennsylvania, Philadelphia, Pennsylvania, USA

<sup>2</sup>Institute of Marine and Coastal Sciences, Rutgers University, New Brunswick, USA

<sup>3</sup>Department of Geosciences, University of Rhode Island, Kingston, Rhode Island, USA

<sup>4</sup>School of Civil and Construction Engineering, Oregon State University, Corvallis, Oregon, USA

<sup>5</sup>School of Forestry and Environmental Studies, Yale University, New Haven, Connecticut, USA

<sup>6</sup>Department of Geology and Astronomy, West Chester University, West Chester, Pennsylvania, USA

<sup>7</sup>Department of Earth and Planetary Sciences, Rutgers University, Piscataway, New Jersey, USA

<sup>8</sup>Department of Physics, University of Toronto, Toronto, Ontario, Canada

Received 10 October 2012; Revised 24 February 2013; Accepted 25 February 2013

**ABSTRACT:** We investigated the effect of tidal-range change and sediment compaction on reconstructions of Holocene relative sea level (RSL) in New Jersey, USA. We updated a published sea-level database to generate 50 sea-level index points and ten limiting dates that define continuously rising RSL in New Jersey during the Holocene. There is scatter among the index points, particularly those older than 7 ka. A numerical model estimated that paleotidal range was relatively constant during the mid and late Holocene, but rapidly increased between 9 and 8 ka, leading to an underestimation of RSL by ~0.5 m. We adjusted the sea-level index points using the paleotidal model prior to assessing the influence of compaction on organic samples with clastic deposits above and below (an intercalated sea-level index point). We found a significant relationship ( $p = 0.01$ ) with the thickness of the overburden ( $r = 0.85$ ). We altered the altitude of intercalated index points using this simple stratigraphic relationship, which reduced vertical scatter in sea-level reconstructions. We conclude that RSL rose at an average rate of  $4 \text{ mm a}^{-1}$  from 10 ka to 6 ka,  $2 \text{ mm a}^{-1}$  from 6 ka to 2 ka, and  $1.3 \text{ mm a}^{-1}$  from 2 ka to AD 1900.

Copyright © 2013 John Wiley & Sons, Ltd.

**KEYWORDS:** sea level; Holocene; sediment compaction; tidal range; index points.

## Introduction

Holocene relative sea level (RSL) on the US Atlantic coast is the product of eustatic, isostatic, tectonic and local contributions. The eustatic function includes the transfer of mass between the ocean and ice sheets, ocean water density (steric) changes from temperature and salinity variations, and gravitational and rotational changes (geoid contribution). Isostasy is the total effect of glacio- and hydro-isostasy. Tectonic contributions are assumed to be localized or negligible for the Holocene (Sykes *et al.*, 2008). Local processes include tidal-range change and sediment compaction.

Sea-level index points are individual reconstructions of sea level with quantified age and vertical uncertainties. Groups of sea-level index points describe trends and patterns in RSL change through time and space. Compiled index points from New Jersey show continuous RSL rise during the Holocene (e.g. Daddario, 1961; Stuiver and Daddario, 1963; Bloom, 1967; Meyerson, 1972; Psuty, 1986; Miller *et al.*, 2009; Engelhart and Horton, 2012). During deglaciation the contribution of global ice melt to sea-level change averaged  $10 \text{ mm a}^{-1}$ , although peak rates exceeded  $47 \text{ mm a}^{-1}$  during meltwater pulse 1a at 14.5 ka (e.g. Deschamps *et al.*, 2012). Empirical data and glacial isostatic adjustment (GIA) models suggest a significant reduction in the eustatic contribution at approximately 7 ka; since when ocean volume changed only by a few meters (Peltier, 1998; Lambeck and Chappell, 2001; Mitrovica and Milne, 2002; Bassett *et al.*, 2005). GIA models

predict that New Jersey is influenced by ongoing subsidence in response to collapse and retreat of the Laurentide Ice Sheet forebulge and the return flow of mantle material towards formerly glaciated areas (Tushingham and Peltier, 1992). The models (e.g. Peltier, 2004; Engelhart *et al.*, 2011) and RSL reconstructions (Psuty, 1986; Miller *et al.*, 2009; Engelhart *et al.*, 2009; Engelhart and Horton, 2012) suggest that the eustatic and isostatic contributions did not vary spatially within New Jersey. RSL predictions from GIA models predictions are similar for sites in northern and southern New Jersey (Fig. 1c) because they are a similar distance to the center of the former Laurentide Ice Sheet in Hudson Bay (Peltier, 2004) and consequently shared the same eustatic and isostatic history. This spatial uniformity is also seen in Holocene sea-level reconstructions, where sea-level index points from Cheesequake in northern New Jersey (Psuty, 1986; Fig. 1a) are in broad agreement with contemporaneous ones from sites in central and southern New Jersey (Engelhart and Horton, 2012). Therefore, the relatively small differences among sites and sea-level index points of the same age are assumed to be a product of local processes.

The contribution of local factors to reconstructed Holocene RSL change in New Jersey is unknown. We analyzed a database of sea-level index points (Engelhart and Horton, 2012) to estimate the influence of tidal-range change and compaction (local processes) on RSL reconstructions from New Jersey. If tidal range changed through time, RSL reconstructions based upon tide-level indicators will differ from the actual sea level (Gehrels *et al.*, 1995; Shennan *et al.*, 2000b; Shennan and Horton, 2002; Hall *et al.*, 2013). We use a numerical paleotidal model (Hill *et al.*, 2011) that

\*Correspondence: B. P. Horton, <sup>2</sup> Institute of Marine and Coastal Sciences, as above.

Email: bphorton@marine.rutgers.edu

predicts temporal variations in tidal range to modify the vertical uncertainty of individual index points. Compaction reduces sediment volume by rearrangement of the mineral matrix and biodegradation (Kaye and Barghoorn, 1964; Allen, 2000; Brain *et al.*, 2011). This process lowers the altitude of the land surface (Cahoon *et al.*, 2002), causing samples used for RSL reconstruction to have a lower elevation compared to where they formed (e.g. Brain *et al.*, 2012). We suggest that there was a significant change in tidal range in the early Holocene and demonstrate that compaction was a considerable driver of RSL change in New Jersey with deviations of up to 10 m from the regional RSL record. The application of a first-order method of decompaction based on the stratigraphic position of index points reduces vertical scatter in the reconstructions.

## Sea-level index points

Sea-level index points are estimates of the position of RSL in space and time. Engelhart and Horton (2012) produced a standardized database of Holocene sea-level index points from published literature for the US Atlantic coast. Salt marshes provided all sea-level index points (basal and intercalated) in the New Jersey database. Individual index points are presented as boxes that incorporate estimated age and vertical uncertainty. Each index point possessed the following:

1. *Location*: consisting of its geographical coordinates.
2. *Radiocarbon age (and uncertainty)*: calibrated using CALIB 6.1 (Reimer *et al.*, 2009) with a  $2\sigma$  error, where zero is AD 1950. In this paper, we expressed the unit for thousands of years as 'ka', both for ages and time spans.
3. *Elevation (and uncertainty)*: RSL was reconstructed using sea-level indicators and their indicative meaning that was defined from analogous modern examples. The indicative meaning describes the relationship of a sea-level indicator to elevation in the tidal frame and is comprised of a mid-point that is a tidal datum (the reference water level) and a vertical range (the indicative range). This approach allows

samples of varied origins to be plotted together as a single RSL curve. We estimated three indicative meanings for salt marsh samples (Table 1) from the zonation of vegetation and assemblages of microfossils, and  $\delta^{13}\text{C}$  values of bulk sediment (Kemp *et al.*, 2012a, 2012b). RSL is calculated by subtracting the reference water level from sample altitude. Engelhart and Horton (2012) calculated a vertical error for each index point from the indicative range and factors inherent in the collection and processing of samples for sea-level research (e.g. surveying, angle of borehole, sample thickness).

## Tidal-range change

If tidal range was greater in the past, the reference water-level value would be greater and consequently RSL would be lower. Therefore, failing to account for tidal-range increase would lead to an underestimation of the true magnitude of RSL change. Paleotidal data for New Jersey were predicted using a nested modeling approach. Complete details are available in Hill *et al.* (2011) and Hall *et al.* (2013), and only a brief overview is presented here. A global tidal model (Griffiths and Peltier, 2008, 2009), including self-attraction and loading, drag in shallow seas and internal tide drag, was first used to compute tidal constituent amplitudes and phases on an  $800 \times 800$  regular grid. At this resolution, the grid spacing varies smoothly from about 50 km in the Tropics to about 5 km around the coast of Greenland. The results from the global model forced the open boundary of a regional tidal model spanning the western Atlantic Ocean, the Gulf of Mexico and the Caribbean Sea. The regional model (ADCIRC; Luettich and Westerink, 1991) used an unstructured finite-element computational mesh that allows for variable spatial resolution. The mesh for the present study had roughly 500 000 elements with nearshore resolution of 1–2 km. This resolution was sufficient to retain many coastal embayments and estuaries, though other very small features were filtered out. To validate its use, data were computed at approximately 250 NOAA tide-gauge locations on the US Atlantic and Gulf coasts (from Maine to Texas). Hill *et al.* (2011) showed a very

**Table 1.** Summary of the indicative meanings used to generate the basal and intercalated sea-level index points of the New Jersey database.

Sample type	Evidence	Reference water level	Indicative range
High marsh environment	High marsh plant macrofossils (e.g. Kemp <i>et al.</i> , 2012a). Foraminiferal (e.g. Kemp <i>et al.</i> , 2012b) assemblages dominated by high marsh taxa	(HAT-MHW)/2	HAT-MHW
Low marsh environment	Low marsh plant macrofossils (e.g. Kemp <i>et al.</i> , 2012a). Foraminiferal assemblages dominated by low marsh taxa (e.g. Kemp <i>et al.</i> , 2012b)	(MHW-MTL)/2	MHW-MTL
Undifferentiated salt marsh environment	Author listing of unnamed salt marsh plant macrofossils or identification only to genus level (e.g. Donnelly <i>et al.</i> , 2001, 2004). Foraminiferal assemblages dominated by high and low marsh taxa (e.g. Kemp <i>et al.</i> , 2012b). Diatom assemblage dominated by brackish and or marine taxa (e.g. Cinquemani <i>et al.</i> , 1982)	(HAT-MTL)/2	HAT-MTL
Marine limiting	Identifiable <i>in situ</i> marine shells (e.g. Psuty <i>et al.</i> , 1986) or calcareous foraminiferal assemblages (e.g. Miller <i>et al.</i> , 2009) in clastic sediment	MTL	Below MTL
Terrestrial limiting	Peat that does not meet the above requirements to be classified as an index point (e.g. Psuty <i>et al.</i> , 1986)	MTL	Above MTL

MHW, mean high water; MTL, mean tide level; HAT, highest astronomical tide.

good agreement between the NOAA tide-gauge observations and independent model predictions. The correlation coefficient ( $r$ ) between the two sets of mean higher high water values was 0.93.

For paleobathymetries, depth changes from the ICE-5G GIA model of Peltier (2004) were interpolated on to the regional grid. Tidal amplitudes and phases (obtained from harmonic analysis of the regional model results) were converted to tidal data using the harmonic constant datum method of Mofjeld *et al.* (2004). The paleotidal models do not include the effects of sediment infilling of estuaries and coastal lowlands or freshwater discharge from the catchments (Shennan *et al.*, 2000b).

The reference water level and indicative range for all index points were corrected for the local tidal conditions that prevailed at the time of sample deposition using hindcasts from the paleotidal model. Computational runs were carried out at 1 ka intervals from 10 ka to present day. Following Hill *et al.* (2011), the percentage change in each tidal datum between present day and the model runs was used to provide the absolute values. Data at locations other than the model grid points (i.e. sites with index points; Fig. 1a) were obtained through interpolation. However, some nodes that were in close proximity to the coastline at a given time interval would alternate between wet and dry during the tidal cycle. This intermittent submergence adversely affected the harmonic analysis at these locations. To address this, data at these nodes were first replaced with mean values from neighboring nodes. Then, a surface-fitting algorithm computed data on a high-resolution rectangular grid, based on the scattered data from the finite-element mesh. This grid was allowed to extend shoreward of the coastline at any given time slice, in order to extrapolate results to locations of interest.

**Sediment compaction**

Sea-level index points may have undergone post-depositional displacement in altitude due to compaction of underlying sediment. This is a one directional process that can only lower altitude in comparison to where the sample was originally deposited, resulting in an RSL reconstruction that is too low. Subdivision of index points into basal and intercalated categories provides an initial assessment of the influence of compaction (Shennan and Horton, 2002; Horton and Shennan, 2009). Intercalated samples are derived from easily compressible organic sediment with clastic units above and below in the sedimentary column (Shennan and Horton, 2002). Basal samples are from an organic sedimentary unit that directly overlays a relatively incompressible substrate (Jelgersma, 1961). Therefore, the influence of sediment compaction for basal samples is minor compared to index points from peat intercalated between thick Holocene clastic sediments (Jelgersma, 1961; Kaye and Barghoorn, 1964). Compaction of intercalated index points can be estimated from three stratigraphical parameters commonly reported in, or estimated from, the original publication: (i) thickness of sediment overburden; (ii) depth to incompressible substrate; and (iii) thickness of the whole sedimentary sequence. We do not account for variation in sediment types, including the proportion of different grain size distributions, organic content, water content or drainage histories, because this information is fragmentary in the original literature for both reporting and methodology.

Compaction of intercalated samples was estimated by modifying RSL predictions (Engelhart *et al.*, 2011) from the ICE-6G VM5b model to fit the basal index points after adjustment for paleotidal changes. It was necessary to use a

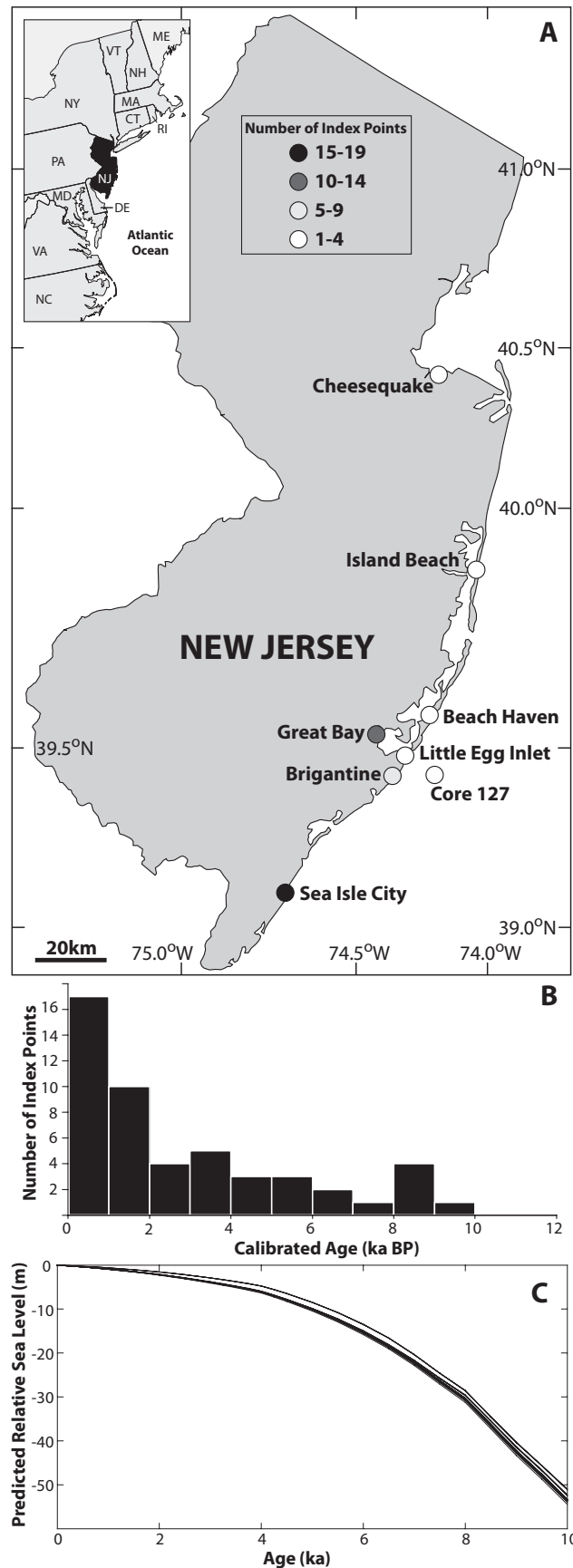


**Figure 1.** (A) Location of sites where sea-level index points were generated. (B) Temporal distribution of sea-level index points from New Jersey. (C) Holocene sea-level predictions of the ICE-6G VM5b (Engelhart *et al.*, 2011) for each of the study sites of New Jersey where sea-level index points were generated.

curve to ensure that all intercalated index points had a contemporary estimate of compaction-free RSL. The vertical difference between each intercalated index point (at its center without consideration of age or vertical uncertainty) and the fitted RSL curve is attributed entirely to sediment compaction. Correlation coefficients were used to compare this residual to the three readily available stratigraphic parameters to test for statistical significance (Shennan *et al.*, 2000a; Horton and Shennan, 2009). Following Edwards (2006), we used the linear regression between the residual and the significant stratigraphic parameters to 'decompact' the intercalated index points. Decompression will elevate the altitude of index points and move the lower points into closer agreement with the modeled curve (Edwards, 2006).

## Regional sea level, tidal-range change and sediment compaction in New Jersey

The updated New Jersey database includes seven new index points not previously reported (Table 2). There are 50 sea-level index points (Fig. 1a) and ten data points that provide limits on the maximum and minimum elevation of RSL. In contrast to other regions of the US Atlantic coast (Engelhart and Horton, 2012), the temporal distribution of sea-level index points is relatively even, with >25% being of early to mid Holocene age (Fig. 1b). Spatially, however, there are no index points between 39.8° N and 40.4° N latitude and only four index points (#10, 11, 12 and 36) from northern New Jersey (Cheesequake Marsh; Psuty, 1986). These northern index points are not distinguishable from those situated in central and southern New Jersey, demonstrating that they can be meaningfully combined into a single RSL region (Fig. 4).

### Influence of paleotidal-range change

RSL changes affect shelf width and bathymetric depths, and consequently change the reflection and amplification of tidal waves and the distribution of frictional dissipation of the tidal energy that is transferred from the deep oceans to the shallow shelf regions (e.g. Hinton, 1992; Shennan *et al.*, 2000b; Uehara *et al.*, 2006; Hill *et al.*, 2011). Today, the Great Diurnal Range (GT) in New Jersey is microtidal (<2 m), with offshore regions <0.8 m. GT is the difference between mean higher high water and mean lower low water (NOAA, 2000).

Paleotidal modeling indicates that GT tripled between 9 ka and 8 ka at the basin-wide scale (Fig. 2). Uehara *et al.* (2006) and Hill *et al.* (2011) attributed it to a combination of the quasi-resonant condition of the Atlantic basin with respect to the semi-diurnal frequency, the opening the Hudson Strait in the early Holocene and the changing extent of the continental shelf. In the mid Holocene tides were amplified south of Long Island (northern New Jersey), likely because of shelf resonance. Based upon present-day bathymetry, the shelf width southeast of Long Island is shorter than a quarter tidal wavelength (~150 vs. 250 km). At 5 ka (Hill *et al.*, 2011), shelf depths in that region were approximately 25 m less, reducing the quarter wavelength of the semi-diurnal tide by ~75 km, bringing it into much closer proximity to the shelf width, and enhancing resonance. GT in the lower Delaware Bay remained fairly constant through time, but ranges in the upper bay doubled from ca. 4 ka to present because the Bay evolved steadily from a narrow river to a funnel-shaped bay. Funnel-shaped estuaries amplify tides with up-bay distance, primarily due to nonlinear overtides (e.g. Parker, 1991).

Changes in tidal range would not affect all types of sea-level index points (high marsh, low marsh, undifferentiated

marsh) evenly (Fig. 3a, b). The reference water level of a hypothetical high-marsh deposit from Brigantine, NJ, at 9 ka would be 1 m higher relative to the present day, and thus RSL 1 m lower. The increase in the indicative range is minor ( $\pm 0.04$  m), because the relationship between highest astronomical tide and mean high water remains near constant through time. The reference water-level increase for Brigantine at 9 ka is reduced (0.5 m) but with larger error terms ( $\pm 0.5$  m) for hypothetical low marsh or undifferentiated salt marsh samples. The reference water level of a hypothetical high-marsh deposit from Brigantine (Fig. 1a) at 9 ka would be 1 m higher than a modern high-marsh deposit, and thus reconstructed RSL would be 1 m lower. The increase in the indicative range is minor ( $\pm 0.04$  m), because the relationship between highest astronomical tide and mean high water remains near constant through time. The reference water-level increase for Brigantine at 9 ka is less (0.5 m) for hypothetical low marsh or undifferentiated salt marsh samples, but with larger changes in the absolute indicative range ( $\pm 0.5$  m). Despite the changes in paleotides (particularly between 9 and 8 ka) the absolute change for a salt marsh sea-level indicator from New Jersey is relatively small due to the modern micro-tidal regime. The maximum decrease in RSL (0.52 m; index point #40) and increase in error ( $\pm 0.31$  m; index points #13 and 14) in the database is small compared to the >20 m of RSL rise observed during the Holocene in New Jersey (Fig. 3c).

### Influence of sediment compaction

The effects of compaction on RSL reconstructions over millennial timescales have been assessed through regional (e.g. Shennan *et al.*, 2000a; Edwards, 2006; Törnqvist *et al.*, 2008; Horton and Shennan, 2009) and local (e.g. Gehrels, 1999; Long *et al.*, 2006) datasets. In New Jersey, intercalated index points record comparable or lower RSL than the curve fitted to basal index points (Fig. 4a). An intercalated index point (#40) at 8.5 ka suggests RSL (after paleotidal correction) was  $-30.7 \pm 1.8$  m, which is more than 10 m lower than basal index points of similar age. The intercalated index point was from Little Egg Inlet and identified as a salt marsh peat by microfossil and palynological analysis (Field *et al.*, 1979). In the Late Holocene there are six intercalated index points with 1–4 m differences in RSL compared to basal index points, with the oldest (#39) plotting below a marine limiting date (Miller *et al.*, 2009). In eastern England, Horton and Shennan (2009) showed differences of up to 6 m between basal and intercalated index points of similar age at individual sites. Similarly, Long *et al.* (2006) identified 2–3 m RSL differences between late Holocene basal and intercalated index points deposited in southern England. In the Mississippi Delta, USA, Törnqvist *et al.* (2008) observed >2 m variation in elevation of an isochronous 1.4 ka peat that was overlain with clastic material of variable thickness.

Comparison of the residuals between intercalated index points and the RSL curve fitted to basal data demonstrates that there is a strong ( $r=0.64$ ) and significant (at the 1% level) relationship between the overburden of the sample and the magnitude of the residual (Fig. 4b). The intercalated index point from Little Egg Inlet again plots as outlier. Little Egg Inlet was dredged during the 20th century and is also a location of significant sand mining by New Jersey Department of Environmental Protection (Byrnes *et al.*, 2004). Both processes remove sediment overburden and likely make the measured thickness of overlying sediment an underestimate. Removing this index point from the analyses improves the relationship between the thickness of the overburden and

**Table 2.** Summary of sea-level index points and limiting data from the New Jersey database.

Index points	Location	Longitude	Latitude	Labcode	<sup>14</sup> C age ± 1σ	Calibrated age range	Tidal range correctn (m)	Compcn correctn (m)	RSL (m)	Citation	Code
Index points (Basal)											
1	Beach Haven Inlet	-74.250	39.470	848-26	7790 ± 130	8987-8387	-0.38		-20.55 ± 1.70	Strahl <i>et al.</i> (1974)	3
2	Beach Haven Inlet	-74.250	39.470	833-25	7860 ± 190	9256-8334	-0.38		-20.55 ± 1.70	Strahl <i>et al.</i> (1974)	3
3	Beach Haven Inlet	-74.250	39.470	816-35	8210 ± 120	9481-8779	-0.38		-21.55 ± 1.70	Strahl <i>et al.</i> (1974)	3
4	Brigantine Marsh	-74.390	39.426	Y-1284	5890 ± 100	6951-6453	-0.07		-13.02 ± 0.82	Stuiver and Daddario (1963)	3
5	Brigantine Marsh	-74.354	39.420	Unknown	240 ± 50	461-0	0.00		-1.70 ± 0.67	Donnelly <i>et al.</i> (2004)	2
6	Brigantine Marsh	-74.426	39.485	Y-1331	1890 ± 40	1922-1720	-0.02		-2.56 ± 0.77	Stuiver and Daddario (1963)	3
7	Brigantine Marsh	-74.424	39.483	Y-1281	3000 ± 90	3387-2929	0.02		-4.63 ± 0.75	Stuiver and Daddario (1963)	3
8	Brigantine Marsh	-74.419	39.479	Y-1282	3830 ± 100	4517-3929	-0.03		-7.38 ± 0.79	Stuiver and Daddario (1963)	3
9	Brigantine Marsh	-74.405	39.454	Y-1283	4760 ± 80	5642-5315	-0.08		-10.32 ± 0.83	Stuiver and Daddario (1963)	3
10	Cheesequake Marsh	-74.300	40.400	QC-844	1210 ± 185	1509-738	-0.01		-2.63 ± 0.85	Cinquemani <i>et al.</i> (1982)	3
11	Cheesequake Marsh	-74.300	40.400	QC-847	1960 ± 130	2305-1572	0.05		-2.79 ± 0.81	Cinquemani <i>et al.</i> (1982)	3
12	Cheesequake Marsh	-74.300	40.400	QC-842	2080 ± 160	2457-1625	0.05		-3.26 ± 0.80	Cinquemani <i>et al.</i> (1982)	3
13	Core 127	-74.256	39.416	Unknown	7130 ± 100	8170-7749	-0.33		-17.94 ± 0.91	Miller <i>et al.</i> (2009)	3
14	Core 127	-74.256	39.416	Unknown	7690 ± 50	8581-8401	-0.33		-17.69 ± 0.91	Miller <i>et al.</i> (2009)	3
15	Edwin B. Forsythe	-74.418	39.495	OS-70446	319 ± 13	451-308	0.00		-1.52 ± 0.28	This publication	1
16	Edwin B. Forsythe	-74.418	39.495	OS-66518	950 ± 30	926-794	0.00		-2.09 ± 0.28	This publication	1
17	Edwin B. Forsythe	-74.418	39.495	OS-70444	1188 ± 30	1228-1004	0.00		-2.23 ± 0.28	This publication	1
18	Edwin B. Forsythe	-74.418	39.495	OS-70442	1249 ± 13	1263-1147	0.00		-2.43 ± 0.28	This publication	1
19	Edwin B. Forsythe	-74.418	39.495	OS-70443	1502 ± 14	1407-1349	0.00		-2.70 ± 0.28	Kemp <i>et al.</i> (2012a)	1
20	Edwin B. Forsythe	-74.418	39.495	OS-70445	1541 ± 14	1517-1379	0.00		-2.93 ± 0.28	Kemp <i>et al.</i> (2012a)	1
21	Edwin B. Forsythe	-74.418	39.495	OS-66514	1550 ± 25	1521-1383	0.00		-3.07 ± 0.28	Kemp <i>et al.</i> (2012a)	1
22	Great Bay	-74.349	39.561	Unknown	3035 ± 120	3474-2879	0.00		-4.04 ± 0.76	Psuty <i>et al.</i> (1986)	3
23	Great Bay	-74.324	39.522	Unknown	4175 ± 145	5264-4256	-0.09		-8.44 ± 0.84	Psuty <i>et al.</i> (1986)	3
24	Great Bay	-74.324	39.522	Unknown	4495 ± 125	5565-4843	-0.09		-8.44 ± 0.84	Psuty <i>et al.</i> (1986)	3
25	Island Beach	-74.094	39.803	GX-19017	5625 ± 200	6883-5947	-0.20		-10.57 ± 0.84	Miller <i>et al.</i> (2009)	3
26	Sea Island City	-74.700	39.200	QC-850	920 ± 160	1176-559	0.01		-1.30 ± 0.78	Cinquemani <i>et al.</i> (1982)	3
27	Sea Island City	-74.700	39.200	QC-851	2345 ± 100	2714-2149	0.01		-2.80 ± 0.79	Cinquemani <i>et al.</i> (1982)	3
28	Sea Island City- NJ	-74.700	39.200	QC-853	2760 ± 100	3204-2720	0.04		-4.72 ± 0.77	Cinquemani <i>et al.</i> (1982)	3
29	Sea Island City	-74.700	39.200	QC-854	3440 ± 110	3980-3445	0.01		-5.50 ± 0.80	Cinquemani <i>et al.</i> (1982)	3
30	Sea Island City	-74.700	39.200	QC-855	3960 ± 110	4815-4092	0.01		-7.35 ± 0.80	Cinquemani <i>et al.</i> (1982)	3
31	Sea Island City	-74.730	39.180	QC-852	2260 ± 100	2694-1993	0.02		-3.49 ± 0.78	Pardi <i>et al.</i> (1984)	3
Index points (intercalated)											
32	Brigantine Marsh	-74.354	39.420	Unknown	210 ± 50	425-0	0.00	0.37	-0.48 ± 0.67	Donnelly <i>et al.</i> (2004)	3
33	Brigantine Marsh	-74.354	39.420	Unknown	340 ± 40	488-308	0.00	0.40	-0.56 ± 0.67	Donnelly <i>et al.</i> (2004)	3
34	Brigantine Marsh	-74.354	39.420	Unknown	450 ± 50	616-319	0.00	0.33	-0.49 ± 0.67	Donnelly <i>et al.</i> (2004)	3
35	Brigantine Marsh	-74.354	39.420	Unknown	1420 ± 40	1386-1284	-0.01	0.87	-1.74 ± 0.68	Donnelly <i>et al.</i> (2004)	3
36	Cheesequake Marsh	-74.300	40.400	QC-845	4820 ± 95	5740-5319	-0.11	3.02	-8.04 ± 0.94	Cinquemani <i>et al.</i> (1982)	3
37	Great Bay	-74.320	39.510	OS-34136	1200 ± 35	1257-1009	-0.02	0.68	-0.79 ± 0.28	Miller <i>et al.</i> (2009)	1
38	Great Bay	-74.320	39.510	OS-34134	2890 ± 30	3156-2926	-0.04	1.71	-3.43 ± 0.28	Miller <i>et al.</i> (2009)	1
39	Great Bay	-74.342	39.549	Unknown	3050 ± 95	3448-2972	0.00	2.04	-4.90 ± 0.77	Psuty <i>et al.</i> (1986)	3
40	Little Egg Inlet	-74.123	39.412	GX-2966	7600 ± 300	9239-7799	-0.52	2.06	-28.60 ± 1.78	Field <i>et al.</i> (1979)	1
41	Whale Beach	-74.671	39.184	Beta-129433	60 ± 40	265-0	0.00	0.25	-0.32 ± 0.79	Donnelly <i>et al.</i> (2001)	2
42	Whale Beach	-74.671	39.184	Beta-129432	110 ± 40	273-0	0.00	0.29	-0.37 ± 0.79	Donnelly <i>et al.</i> (2001)	2
43	Whale Beach	-74.671	39.184	Beta-129430	180 ± 40	301-0	0.00	0.47	-0.85 ± 0.79	Donnelly <i>et al.</i> (2001)	2
44	Whale Beach	-74.671	39.184	Beta-128149	210 ± 40	420-0	0.00	0.25	-0.30 ± 0.79	Donnelly <i>et al.</i> (2001)	2
45	Whale Beach	-74.671	39.184	Beta-131490	220 ± 40	425-0	0.00	0.29	-0.37 ± 0.79	Donnelly <i>et al.</i> (2001)	2
46	Whale Beach	-74.671	39.184	Beta-131489	230 ± 40	428-0	0.00	0.36	-0.58 ± 0.79	Donnelly <i>et al.</i> (2001)	2
47	Whale Beach	-74.671	39.184	Beta-124176	290 ± 50	490-0	0.00	0.35	-0.54 ± 0.79	Donnelly <i>et al.</i> (2001)	2
48	Whale Beach	-74.671	39.184	Beta-124177	300 ± 40	474-289	0.00	0.32	-0.47 ± 0.79	Donnelly <i>et al.</i> (2001)	2
49	Whale Beach	-74.671	39.184	Beta-123305	560 ± 50	652-513	0.00	0.45	-0.82 ± 0.79	Donnelly <i>et al.</i> (2001)	2
50	Whale Beach	-74.671	39.184	OS-26451	680 ± 30	680-561	0.00	0.90	-1.95 ± 0.79	Donnelly <i>et al.</i> (2001)	2
Marine limiting											
1	Cheesequake Marsh	-74.273	40.439	Unknown	4330 ± 460	5445-3124			-10.29 ± 0.58	Psuty <i>et al.</i> (1986)	3
2	Rainbow Island I	-74.585	39.305	GX-30879	2580 ± 30	2235-1921			-4.54 ± 0.14	Miller <i>et al.</i> (2009)	4
3	Rainbow Island I	-74.585	39.305	GX-30880	2880 ± 30	2645-2314			-5.15 ± 0.14	Miller <i>et al.</i> (2009)	4
4	Rainbow Island II	-74.588	39.304	GX-31527	2330 ± 70	1956-1561			-3.60 ± 0.14	Miller <i>et al.</i> (2009)	4
5	Rainbow Island II	-74.588	39.304	GX-31528	2980 ± 40	2719-2390			-4.05 ± 0.14	Miller <i>et al.</i> (2009)	4
Terrestrial limiting											
1	Cheesequake Marsh	-74.281	40.435	Unknown	6020 ± 215	7413-6403			-7.59 ± 0.58	Psuty <i>et al.</i> (1986)	2
2	Cheesequake Marsh	-74.273	40.439	Unknown	6610 ± 215	7929-7020			-10.99 ± 0.58	Psuty <i>et al.</i> (1986)	2
3	Cheesequake Marsh	-74.300	40.400	QC-896	7320 ± 185	8508-7756			-11.24 ± 0.58	Cinquemani <i>et al.</i> (1982)	3
4	Cheesequake Marsh	-74.273	40.439	Unknown	7735 ± 195	9086-8163			-11.79 ± 0.58	Psuty <i>et al.</i> (1986)	3
5	Union Beach	-74.161	40.446	Unknown	660 ± 110	896-497			-0.59 ± 0.57	Psuty <i>et al.</i> (1986)	3

Relative sea level (RSL) is calculated by subtracting the reference water level from sample altitude, shown to two decimal places. A correction for tidal range change is applied to basal and intercalated index points. A correction for compaction is applied to intercalated index points. The RSL error range is calculated as the square root of the sum of squares of elevational error, sample thickness, tide-level error and indicative range, shown to two decimal places. The indicative range (given as a maximum) is the most probable vertical range in which the sample occurs, but for marine and terrestrial limiting dates the sample could occur below or above this range, respectively. Every index point for the New Jersey sea-level database has been age dated using radiocarbon techniques and calibrated using CALIB 6.1 (Reimer *et al.*, 2009) with a 2σ error, where zero is AD 1950. We include a code indicating the main line of evidence that led to the classification as an index point (1, 2, 3), terrestrial limiting (2, 3) or marine limiting (3, 4) date (1 = microfossils, 2 = plant macrofossils, 3 = author listing, 4 = identified estuarine/marine shells or foraminifera).

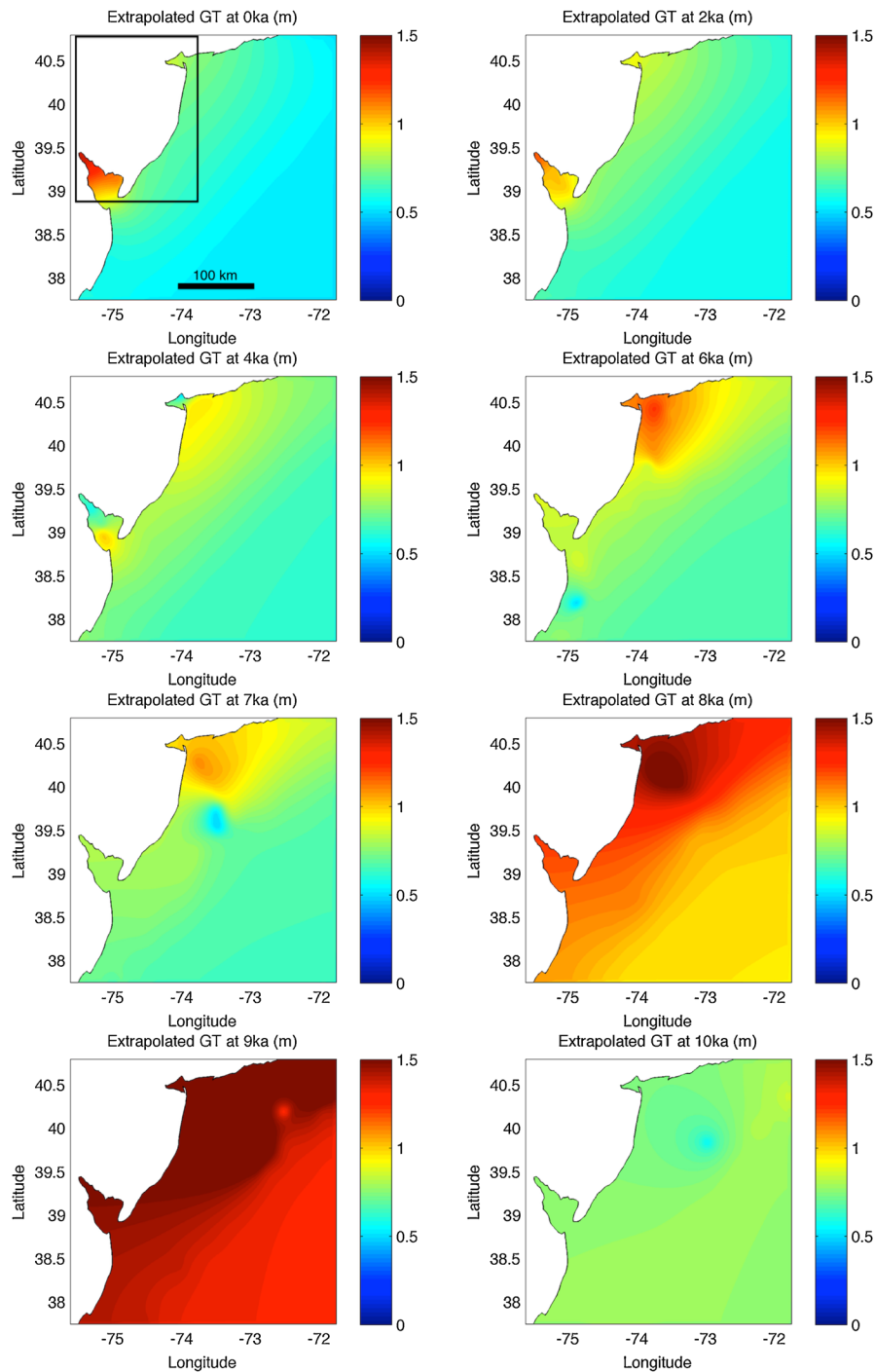


**Figure 2.** Contours of Great Diurnal Range (GT) at selected times during the Holocene. Panel showing GT at 0 ka shows the approximate area of Fig. 1 where the sea-level index points were generated.

residuals ( $r=0.85$ ). There is no relationship (at the 1% level) between the depth to basement (Fig. 4c) and total sediment thickness (Fig. 4d) and residuals.

While the intercalated index point dataset is of limited size, these results are consistent with previous studies from the UK (e.g. Shennan *et al.*, 2000a; Edwards, 2006; Horton and Shennan, 2009) and the US Gulf coast (Törnqvist *et al.*, 2008) and suggest that sediment compaction produces vertical scatter in RSL data. We used the linear regression between residuals and depth of overburden (with the outlying Little Egg Inlet index point excluded) to 'decompact' the intercalated index points (Edwards, 2006). This first-order decompaction procedure elevates the intercalated index points by as much as 3 m and moves them into much closer agreement

with the basal index points and modeled curve. This procedure reduces the vertical scatter among index points.

### *Holocene sea-level history*

The tidal range and sediment compaction-corrected sea-level index points from New Jersey show a continuous rise during the Holocene (Fig. 5). If we assume the Little Egg index point at 8.5 ka no longer accurately estimates former RSL, the remaining index points suggest RSL was between  $-18$  and  $-22$  m at 10–8 ka. RSL rose at an average of  $4 \text{ mm a}^{-1}$  from 10 ka to 6 ka when RSL was between  $-8$  and  $-10$  m. RSL rise slowed to  $2 \text{ mm a}^{-1}$  from 6 ka to 2 ka because of the diminishing response of the Earth's mantle to GIA and

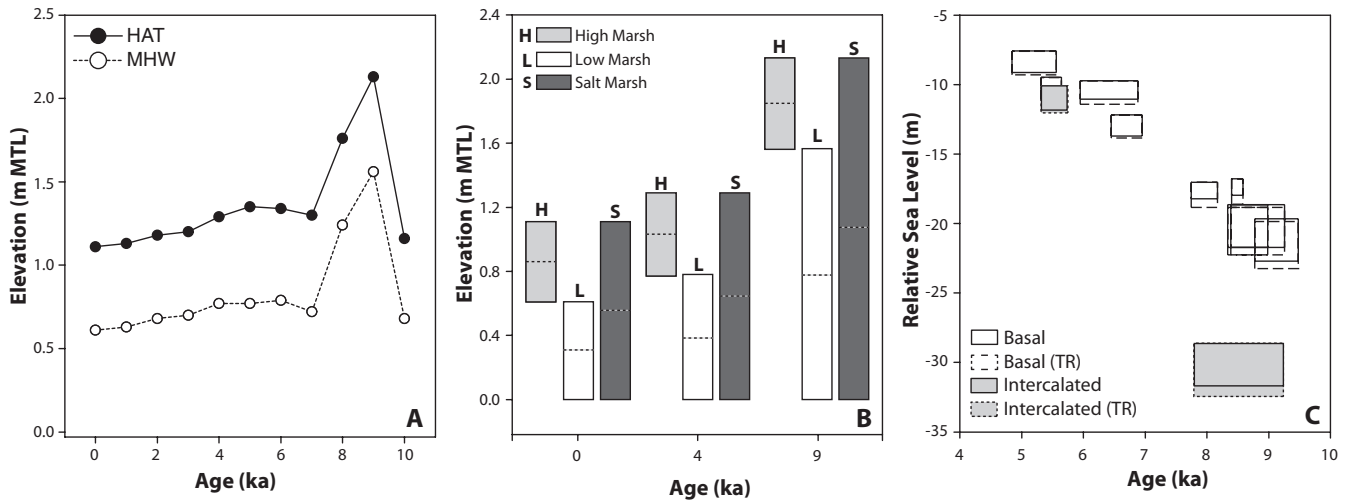


**Figure 3.** (A) Tidal data used to generate the indicative meanings (HAT, highest astronomical tide; MHW, mean high water; MTL, mean tide level) during the Holocene for Brigantine, NJ. (B) Reference water level and indicative range of saltmarsh, high marsh and low marsh at 0, 4 and 9 ka for Brigantine, NJ. (C) Sea-level index points with and without tidal range change correction in the mid and early Holocene.

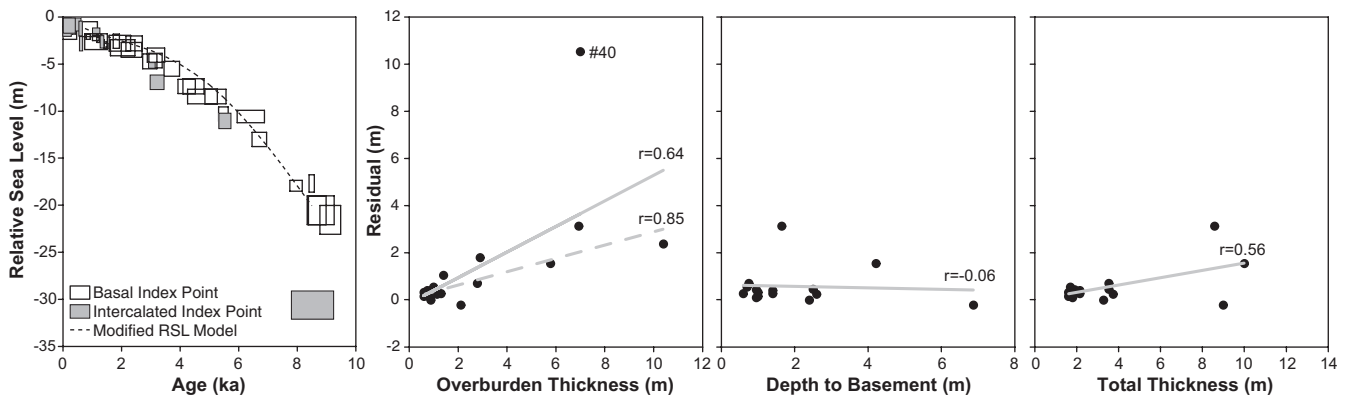


**Figure 4.** Sea-level index points and limiting data subdivided into basal and intercalated and the RSL curve. Overburden, depth to basement and total thickness of sediment versus residual for intercalated index points. 'Residual' is the difference between the fitted RSL curve and the center point of each intercalated index point.

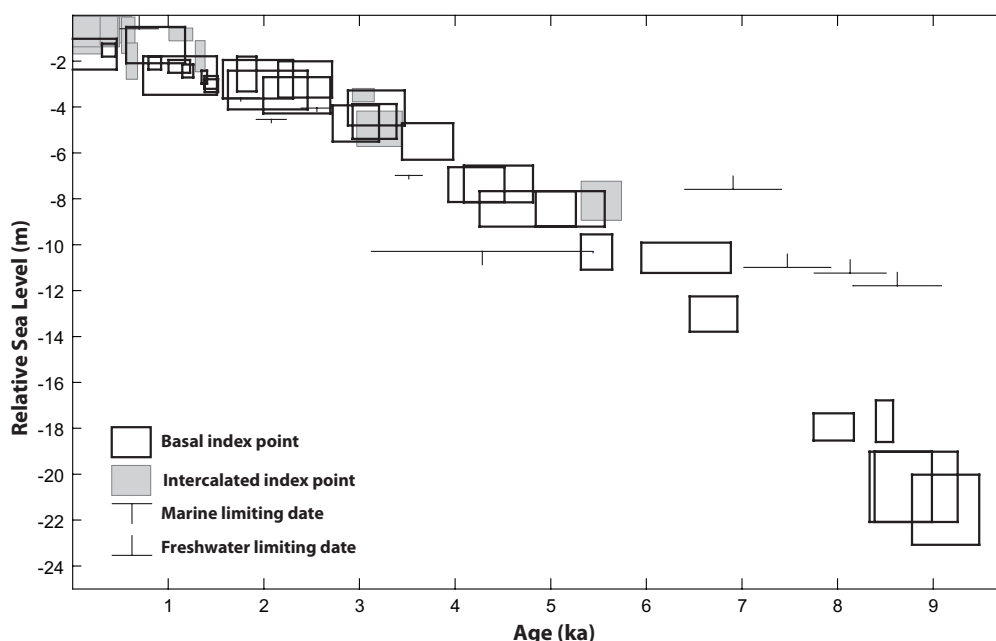


**Figure 5.** Holocene sea-level index points and limiting dates from New Jersey. Decompacted and tidal range corrected basal and intercalated index points are plotted as boxes with  $2\sigma$  vertical and calibrated age errors.

reduction of eustatic input (Milne *et al.*, 2005; Englehart and Horton, 2012). From 2 ka to AD 1900, we calculated a rate of  $1.3 \pm 0.1 \text{ mm a}^{-1}$ , which is almost all due to GIA (Peltier, 1998; Lambeck, 2002; Milne *et al.*, 2005).

## Conclusions

We updated a published Holocene sea-level database to generate 50 sea-level index points and ten limiting dates for New Jersey. Rates of RSL change were highest during the early and mid Holocene and decreased since. Reconstructions of RSL and modeled paleobathymetry for 1 ka time steps through the Holocene predict significant changes in tidal regimes as the transgression of the continental shelf progresses. The most significant changes occur in the upper Delaware Bay during the late Holocene, south of Long Island in the mid Holocene and the basin-wide amplification of the tide at 9–8 ka. However, these paleotidal changes have only minor implications in the analysis of Holocene RSL because of the microtidal regime. In contrast, sediment compaction explains meter-scale variations in elevation of RSL derived from index points taken from basal peat and those from peat intercalated within thick successions of Holocene sediments. We decompacted the intercalated index points using the thickness of sediment overburden, reducing the vertical scatter in sea-level reconstructions.

**Acknowledgements.** Funding for this study was provided by NICRR grant DE-FC02-06ER64298, National Science Foundation awards EAR 0717364, 1052848 and 0951686, NOAA grant NA11OAR4310101 and a Yale Climate and Energy Institute post-doctoral fellowship. This research was supported by the Earthwatch Institute Student Challenge Award Program and we thank the students who participated so enthusiastically in fieldwork. The Edwin Forsythe National Wildlife Refuge (US Fish and Wildlife Service) is acknowledged for their cooperation and for providing access to study sites. We acknowledge the researchers who collected the data, which has subsequently been reanalyzed in this study, and greatly appreciate their assistance and advice throughout this process. We thank Patrick Kiden and an anonymous reviewer, whose comments improved the manuscript. This paper is a contribution to IGCP project 588 'Preparing for coastal change' and PALSEA.

**Abbreviations.** GIA, glacial isostatic adjustment; GT, Great Diurnal Range; RSL, relative sea level

## References

Allen JRL. 2000. Morphodynamics of Holocene salt marshes: a review sketch from the Atlantic and southern North Sea coasts of Europe. *Quaternary Science Reviews* **19**: 1155–1231.

Bassett SE, Milne GA, Mitrovica JX, *et al.* 2005. Ice sheet and solid earth influences on far-field sea-level histories. *Science* **309**: 925–928.

Bloom AL. 1967. Pleistocene shorelines: a new test of isostasy. *Geological Society of America Bulletin* **78**: 1477–1494.

Brain MJ, Long AJ, Petley DN, *et al.* 2011. Compression behavior of minerogenic low energy intertidal sediments. *Sedimentary Geology* **23**: 28–41.

Brain MJ, Long AJ, Woodroffe SA, *et al.* 2012. Modelling the effects of sediment compaction on salt marsh reconstructions of recent sea-level rise. *Earth and Planetary Science Letters* **345–348**: 180–193.

Byrnes MR, Hammer RM, Thibaut TD, *et al.* 2004. Effects of sand mining on physical processes and biological communities offshore New Jersey, U.S.A. *Journal of Coastal Research* **20**: 25–43.

Cahoon DR, Lynch JC, Hensel P, *et al.* 2002. A device for high precision measurement of wetland sediment elevation. I. Recent improvements to the sedimentation–erosion table. *Journal of Sedimentary Research* **72**: 730–733.

Cinquemani LJ, Newman WS, Sperling JA, *et al.* 1982. Holocene sea level fluctuations, magnitudes and causes. IGCP Annual Meeting, Columbia, SC; 13–33.

Daddario JJ. 1961. A lagoon deposit profile near Atlantic City, New Jersey. *Bulletin of the New Jersey Academy of Science* **6**: 7–14.

Deschamps P, Durand N, Bard E, *et al.* 2012. Ice sheet collapse and sea-level rise at the Bølling warming, 14,600 yr ago. *Nature* **483**: 559–564.

Donnelly JP, Roll S, Wengren M, *et al.* 2001. Sedimentary evidence of intense hurricane strikes from New Jersey. *Geology* **29**: 615–618.

Donnelly JP, Butler J, Roll S, *et al.* 2004. A backbarrier overwash record of intense storms from Brigantine, New Jersey. *Marine Geology* **210**: 107–121.

Edwards RJ. 2006. Mid- to late-Holocene relative sea-level change in southwest Britain and the influence of sediment compaction. *Holocene* **16**: 575–587.

Engelhart SE, Horton BP. 2012. Holocene sea level database for the Atlantic coast of the United States. *Quaternary Science Reviews* **54**: 12–25.

Engelhart SE, Horton BP, Douglas BC, *et al.* 2009. Spatial variability of late Holocene and 20th century sea-level rise along the Atlantic coast of the United States. *Geology* **37**: 1115–1118.

Engelhart SE, Peltier WR, Horton BP. 2011. Holocene relative sea-level changes and glacial isostatic adjustment of the U.S. Atlantic coast. *Geology* **39**: 751–754.

Field ME, Meisburger EP, Stanley EA, *et al.* 1979. Upper Quaternary peat deposits on the Atlantic inner shelf of the United States. *Geological Society of America Bulletin* **90**: 618–628.

Gehrels WR. 1999. Middle and late Holocene sea-level changes in Eastern Maine reconstructed from foraminiferal saltmarsh stratigraphy and AMS C-14 dates on basal peat. *Quaternary Research* **52**: 350–359.

Gehrels WR, Belknap D, Pearce B, *et al.* 1995. Modeling the contribution of M2 tidal amplification to the Holocene rise of mean high water in the Gulf of Maine and Bay of Fundy. *Marine Geology* **124**: 71–85.

Griffiths SD, Peltier WR. 2008. Megatides in the Arctic Ocean under glacial conditions. *Geophysical Research Letters* **35**: L08605.

Griffiths SD, Peltier WR. 2009. Modeling of polar ocean tides at the Last Glacial Maximum: amplification, sensitivity, and climatological implications. *Journal of Climate* **22**: 2905–2924.

Hall GF, Hill DF, Horton BP, *et al.* 2013. A high-resolution study of tides in the Delaware Bay: past conditions and future scenarios. *Geophysical Research Letters* **40**: 338–342.

Hill DF, Griffiths SD, Peltier WR, *et al.* 2011. High resolution numerical modeling of tides in the western Atlantic, Gulf of Mexico, and Caribbean Sea during the Holocene. *Journal of Geophysical Research* **116**: C10014.

Hinton A. 1992. Paleotidal changes within the area of the Wash during the Holocene. *Proceedings of the Geology Association* **103**: 259–272.

Horton BP, Shennan I. 2009. Compaction of Holocene strata and the implications for relative sea-level change on the east coast of England. *Geology* **37**: 1083–1086.

Jelgersma S. 1961. Holocene sea-level changes in the Netherlands. *Mededelingen Geologische Stichting Serie C VI*: 1–100.

Kaye CA, Barghoorn ES. 1964. Late Quaternary sea-level change and crustal rise at Boston, Massachusetts, with notes on the autocompaction of peat. *Geological Society of America Bulletin* **75**: 63–80.

Kemp AC, Vane CH, Horton BP, *et al.* 2012a. Application of stable carbon isotopes for reconstructing salt-marsh floral zones and relative sea level, New Jersey, USA. *Journal of Quaternary Science* **27**: 404–414.

Kemp AC, Horton BP, Vann DR, *et al.* 2012b. Quantitative vertical zonation of salt-marsh foraminifera for reconstructing former sea level: an example from New Jersey, USA. *Quaternary Science Reviews* **54**: 26–39.

Lambeck K. 2002. Sea level change from mid-Holocene to recent time: an Australian example with global implications. In *Ice Sheets, Sea Level and the Dynamic Earth*, Mitrovica JX, Vermeersen BLA (eds.). AGU: Washington, DC; 33–50.



- Lambeck K, Chappell J. 2001. Sea level change through the last glacial cycle. *Science* **292**: 679–685.
- Long AJ, Waller MP, Stupples P. 2006. Driving mechanisms of coastal change: peat compaction and the destruction of late Holocene coastal wetlands. *Marine Geology* **225**: 63–84.
- Luettich R, Westerink J. 1991. A solution for the vertical variation of stress, rather than velocity, in a three-dimensional circulation model. *International Journal for Numerical Methods in Fluids* **12**: 911–928.
- Meyerson AL. 1972. Pollen and paleosalinity analysis from a Holocene tidal marsh sequence, Cape May County, New Jersey. *Marine Geology* **12**: 335–357.
- Miller KG, Sugarman PJ, Browning JV, et al. 2009. Sea-level rise in New Jersey over the past 5000 years: implications to anthropogenic changes. *Global and Planetary Change* **66**: 10–18.
- Milne GA, Long AJ, Bassett SE. 2005. Modelling Holocene relative sea-level observations from the Caribbean and South America. *Quaternary Science Reviews* **24**: 1183–1202.
- Mitrovica JX, Milne GA. 2002. On the origin of late Holocene sea-level highstands within equatorial ocean basins. *Quaternary Science Reviews* **21**: 2179–2190.
- Mofjeld H, Venturato A, Gonzales F, et al. 2004. The harmonic constant datum method: options for overcoming datum discontinuities at mixed-diurnal tidal transitions. *Journal of Atmospheric and Oceanic Technology* **21**: 95–104.
- NOAA. 2000. *Special Publication NOS CO-OPS 1: Tidal Datums and their Applications*. NOAA: Silver Spring, MD.
- Pardi RR, Tomecek L, Newman WS. 1984. Queens college radiocarbon measurements IV. *Radiocarbon* **26**: 412–430.
- Parker BB. 1991. The relative importance of the various non-linear mechanisms in a wide range of tidal interactions. In *Tidal Hydrodynamics*, Parker BB (ed.). Wiley: New York; 237–268.
- Peltier WR. 1998. Postglacial variations in the level of the sea: implications for climate dynamics and solid-earth geophysics. *Reviews of Geophysics* **36**: 603–689.
- Peltier WR. 2004. Global glacial isostasy and the surface of the ice-age Earth: the ICE-5G(VM2) model and GRACE. *Annual Review of Earth and Planetary Science* **32**: 111–149.
- Psuty NP. 1986. Holocene sea level in New Jersey. *Physical Geography* **7**: 156–167.
- Reimer PJ, Baillie MGL, Bard E, et al. 2009. IntCal09 and Marine09 radiocarbon age calibration curves, 0–50,000 years cal BP. *Radiocarbon* **51**: 1111–1150.
- Shennan I, Horton BP. 2002. Holocene land- and sea-level changes in Great Britain. *Journal of Quaternary Science* **17**: 511–526.
- Shennan I, Lambeck K, Horton BP, et al. 2000a. Holocene isostasy and relative sea-level changes on the east coast of England Special Publication 166. Geological Society: London; 275–298.
- Shennan I, Lambeck K, Flather R, et al. 2000b. Modelling western North Sea palaeogeographies and tidal changes during the Holocene. Special Publication 166. Geological Society: London; 299–319.
- Stahl L, Koczan J, Swift D. 1974. Anatomy of a shoreface-connected sand ridge on the New Jersey shelf: implications for the genesis of the shelf surficial sand sheet. *Geology* **2**: 117–120.
- Stuiver M, Daddario JJ. 1963. Submergence of the New Jersey Coast. *Science* **142**: 951.
- Sykes LR, Armbruster JG, Kim WY, et al. 2008. Observations and tectonic setting of historic and instrumentally located earthquakes in the greater New York City–Philadelphia Area. *Bulletin of the Seismological Society of America* **98**: 1696–1719.
- Törnqvist TE, Wallace DJ, Storms JEA, et al. 2008. Mississippi Delta subsidence primarily caused by compaction of Holocene strata. *Nature Geoscience* **1**: 173–176.
- Tushingham AM, Peltier WR. 1992. Validation of the ICE-3G model of Wurm–Wisconsin deglaciation using a global data-base of relative sea-level histories. *Journal of Geophysical Research: Solid Earth* **97**: 3285–3304.
- Uehara K, Scourse JD, Horsburgh JK, et al. 2006. Tidal evolution of the northwest European shelf seas from the Last Glacial Maximum to the present. *Journal of Geophysical Research* **111**: no. C9.